Dynamics of Continuous, Discrete and Impulsive Systems
Series **B:** *Applications & Algorithms* **14 (S8) (2007)** 149-165
 http://www.watam.org

RECENT DEVELOPMENT ON FLUID-STRUCTURE INTERACTION CONTROL BASED ON SURFACE PERTURBATION

M.M. Zhang, L. Cheng and Y. Zhou*

Department of Mechanical Engineering
The Hong Kong Polytechnic University
Hom, Kowloon, Hong Kong
*E-mail: mmyzhou@polyu.edu.hk

Abstract. Control of fluid-structure interactions has been extensively investigated in the past. Various techniques have been developed, including passive control techniques such as changing structural geometries, adding grooves, shrouds or near-wake stabilizers to structures and active control techniques such as acoustic excitation, oscillating or rotating structures and surface bleeding. A novel surface perturbation technique has emerged recently, which has been successfully applied to control flow, flow-induced vibration and noise. In this article, we summarize this technique, major applications, control performances, and possible physical mechanisms responsible for flow modification, drag reduction, controlling fluctuating forces/structural vibrations, and noise control.

Keywords. Perturbation-based control technique, active control, fluid-structure interaction, vortex shedding, flow-induced vibration, flow-induced noise.

AMS (MOS) subject classification: 93C73, 76B75, 74F10, 76B47, 74H45, 60H99.

1 Introduction

A uniform cross flow over a bluff body forms the boundary layer around the body. The boundary layer may separate alternately from either side of the body, forming an alternate Kámán vortex street, when the Reynolds number Re ($\equiv U_\infty h/\nu$, where U_∞ is the free-stream velocity; h the characteristic height of a structure and ν the kinematic viscosity of the fluid) exceeds a critical value [1]. Vortex shedding alternately from the two sides of the body produces a fluctuating pressure on the body, subsequently giving rise to excitation forces and causing the structure to vibrate. The structural motion in turn influences the flow field, resulting in a highly nonlinear fluid-structure coupling [2, 3]. Vortex shedding is also responsible for noise generation in case the kinetic energies of vortical motions are converted into the acoustic wave involving the longitudinal oscillation of fluid particles [4]. Flow-induced vibration may affect the fatigue life of engineering structures (e.g. off-shore structures, high-rise buildings, cable-stayed bridges, and fluid machinery) and even lead to structural damages and serious accidents, and have become one of major concerns in many applications. Therefore, the control of flow and its induced structural vibration has attracted the interests of many researchers for many years.

A variety of control techniques have been developed in the past, which can be roughly classified as passive and active controls. The former, requiring no external energy, often takes effect on flow by changing structural geometries, adding grooves, shrouds or near-wake stabilizers to structures [5, 6]. The later involves energy input via the use of actuators to bring about desirable changes to the fluid-structure system using either an independent external disturbance, i.e. the open-loop control, or a feedback system, i.e. the closed-loop control. Most of previous active control techniques aim at controlling vortex shedding. Blevins [7] explored the influence of a transverse sound wave on vortex shedding from cylinders at Re from 20000 to 40000. The acoustic wave was emitted from two loudspeakers mounted on the two sides of a wind tunnel test section. It was found that the sound introduced could increase the coherence of vortices along the cylinder axis and cause vortex shedding to be locked on with the excitation acoustic wave. Inspired by this idea, Roussopoulos [8] and Ffowcs-Williams and Zhao [9] used a closed-loop method with the feedback signal from a hot wire to drive loudspeakers. The acoustic excitation from the loudspeakers suppressed vortex shedding from a cylinder at Re = 120 and 400, respectively. Another approach is to control the rollup motion of shear layers separated from a cylinder by oscillating or rotating the cylinder. Using this technique, Warui and Fujisawa [10] and Tokumaru and Dimotakis [11] effectively reduced the vortex strength using the electromagnetic actuators, controlled by a feedback signal from a hot wire placed in the wake (Re $\approx$ 104), installed at both ends of a circular cylinder to create a cylinder motion. William et al [12] developed a surface bleeding technique. By means of blowing and sucking flow through the holes or slots on the surface of cylinders, both symmetrical and anti-symmetrical forcing was introduced into a water flow (Re = 470) at a frequency of about twice the vortex shedding frequency (f_s) through two rows of holes located at $\pm 45^\circ$, respectively, away from the forward stagnation line of the cylinder. They managed to modify f_s and the vortex structure. Baz and Kim [13] and Tani et al [14] used piezo-ceramic actuators installed inside a cantilevered cylinder to exert a force on the cylinder. The actuators were excited by a feedback signal measured from the structural vibration, thus increasing the damping of the cylinder and effectively reducing the structural vibration at the occurrence of resonance (Re = 17160 $\sim$ 26555), when f_s coincided with the natural frequency, f_n' , of the flow-structure system.

Cheng et al [15] proposed a new technique by creating a local perturbation on one surface of a bluff body immersed in a cross flow using piezo-ceramic actuators. They demonstrated that this perturbation, referred to hereinafter as the surface-perturbation-based control, could alter the fluid-structure interactions, suppressing (or enhancing) vortex shedding or flow-induced structural vibration or both of the two elements, and even reducing noise. Both open- and closed-loop control have been investigated. In this review, we will focus on this technique and its development, summarizing the technique itself, applications, performances and physical mechanisms. To this end, the perturbation-based control technique was first introduced. Then earlier works on the perturbed fluid-structure interaction on a cylinder, with various stiffness and boundary conditions, were discussed. Based on the dis-

cussion of the perturbation-flow-structure interaction, the control mechanism of the perturbation-based control technique was analyzed.

2 Perturbation-based control technique

Steady flow incident on bluff bodies is usually unstable and develops into an unsteady Kámán vortex street. Due to the wake instability, this Kámán vortex street is unstable and depends on its infant form [16]. On the other hand, local perturbation to the flow, when small enough to comply with the linear theory but large relatively to the early wake instability, may grow exponentially [17]. Thus, small local perturbations to the flow may exert significant influence on the unsteady vortices. Although the physics involved is not fully understood, there are strong evidences that weak perturbations can influence vortex shedding in the highly non-linear unsteady wake, and this influence can sometimes be dramatic. There have been reports on vortex shedding control via small local perturbation [12, 18, 19]. Den Hartog [20] and Parker [21] introduced small local perturbation to flow by oscillating cylinder transversely and emitting acoustic waves inside the cylinder, respectively. By doing so, they both discovered the enhancement of vortex shedding. The fact that vortex shedding is sensitive to local perturbation may naturally have an impact upon vortex-induced structural vibration since the former is the excitation source of the later. This necessarily results in the alteration of fluid-structure interaction. From another point of view, if an appropriate local perturbation on the structural surface is created to modify the fluid-structure interaction, both vortex shedding and its induced vibration may be controlled simultaneously. Based on this idea, a surface-perturbation-based control technique was developed and local perturbation imposed on the structural surface was exerted using a new type of advanced piezo-ceramic actuators, called THUNDER (THin layer composite UNimorph piezoelectric Driver and sEnsoR).

THUNDER was developed by NASA Langley Research Center in 1996. To our knowledge, this actuator has so far been used for vibration isolation [22], aeroelastic response control [23] and active noise control [24]. Due to a special fabrication process [25], this type of actuators provides appealing features, such as a displacement larger than conventional piezo-ceramic actuators with acceptable load-bearing capacity. THUNDER is a multi-layer composite in which individual materials with different thermal expansion coefficients are layered on top of each other to form a ”sandwich”, comprising a metal base layer, a piezoelectric layer at the middle and an aluminum foil on the top; an ultrahigh performance hot-melt adhesive, LaRCTM-SI, is applied between the layers [Fig. 1(a)]. After several precise pressure and temperature cycles, these layers are bonded together, resulting in a finished product with the characteristics of bend or curvature [Fig. 1(b)]. Under an applied voltage, the actuator deforms out of plane [Fig. 1(c)]. Specifically, the THUNDER actuators presently used can vibrate at a maximum displacement of about 2 mm within a frequency range up to 2 kHz in the absence of loading.

The embodiment of the actuators is schematically shown in Fig. 2(a). A square

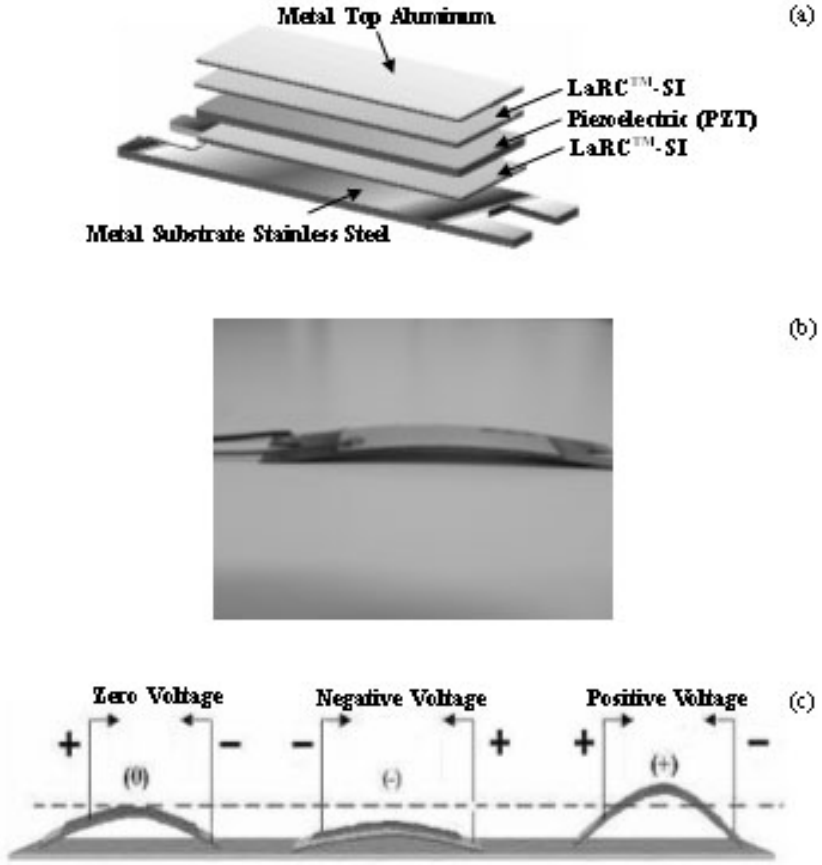

Figure 1. Description of THUNDER actuators: (a) THUNDER construction; (b) photo of THUNDER; (c) typical deformation vs. applied voltage.

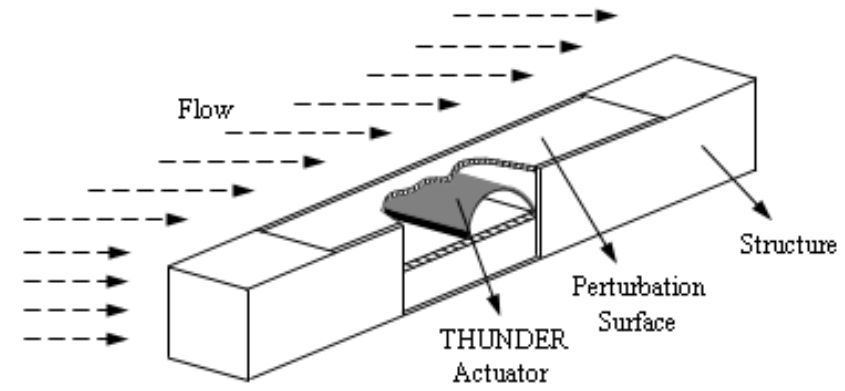

(a)

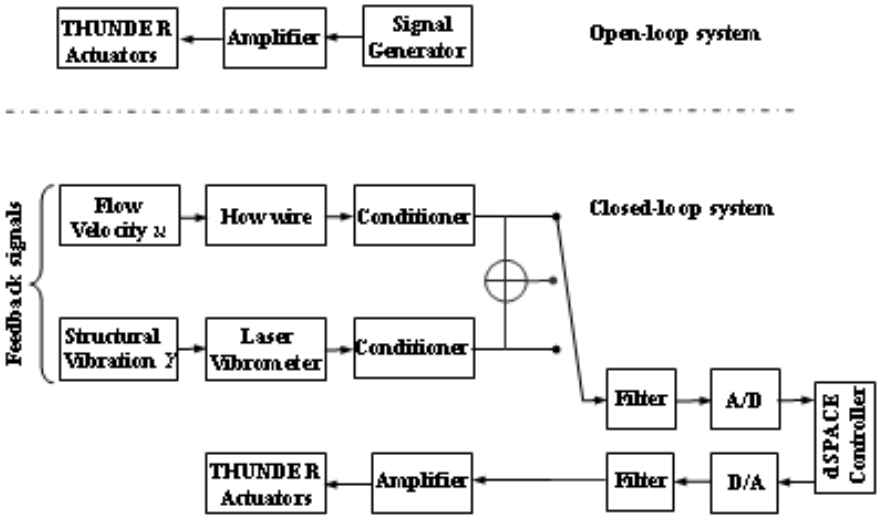

(b)

Figure 2. Embodiment of the perturbation-based control technique: (a) schematic of mechanical configuration; (b) schematic of control system.

test cylinder is used. One thin plate, flush with one cylinder surface, is activated and controlled by a plurality of actuators embedded underneath to oscillate orthogonally to the flow, thus producing a local perturbation to fluid-structure interactions.

It is important that the thin plate should oscillate along with the THUNDER actuators. This was confirmed by tests. Firstly, the plastic plate was removed and the actuators were excited using a sine wave with different frequencies (f_e) and voltages (V_e), generated from a signal generator and amplified by a dual-channel piezo driver amplifier. The displacement of one actuator (Y_a) was measured, simultaneously with the excitation signal, using a laser vibrometer. Two cases were examined. In case I, with f_e fixed at 30 Hz, the root mean square (rms) value of V_e, i.e. $V_{e,rms}$, was set to be 42 volts, 64 volts, 85 volts, 106 volts, 127 volts and 141 volts, respectively. In case II, with $V_{e,rms}$ fixed at 141 volts, f_e was set to be 20 Hz, 40 Hz, 50 Hz and 60 Hz, respectively. $V_{e,rms}$ = 141 volts was the maximum permissible excitation voltage of the actuator. Since the present working frequency of the actuator was less than 60 Hz, experiments were only conducted using a low excitation frequency. Due to space limitation, figure 3(a) only shows the typical time histories of Y_a and excitation signal when f_e and $V_{e,rms}$ are set to be 30 Hz and 127 volts and 50 Hz and 141 volts. Evidently, irrespective of f_e and $V_{e,rms}$, Y_a and excitation signals have similar waveform and are almost in-phased, implying that the phase relationship between the displacements of the plate (Y_p) and Y_a can be approximately thought to be that between Y_p and the excitation signal.

Secondly, the plastic plate was placed on the top of the actuators. Three locations on the surface of the plate at an interval of 164 mm, which was 1/3 of the plate length, were selected and the corresponding displacement of the plate Y_p was measured using the laser vibrometer, again simultaneously with the excitation signal. The same two cases were examined. Figure 3(b) show the typical time histories of Y_p and the excitation signal, corresponding to the three locations, when f_e and $V_{e,rms}$ was set to be 50 Hz and 141 volts, respectively. Evidently, irrespective of $V_{e,rms}$ and f_e, the waveforms of Y_p at each location and the corresponding excitation signal are very similar. Furthermore, the phase shift between Y_p and the corresponding excitation signal is almost the same at the three locations exists given the same f_e and $V_{e,rms}$, as confirmed by measuring the time difference between the wave crest for each signal. The magnitude and waveform of Y_p and Y_a are also the same (Fig. 3). Therefore, two conclusions can be drawn. (1) The movement of the plate is approximately to be uniform along the spanwise direction, suggesting the two-dimensionality of the perturbation. (2) There is a phase shift between the movement of the plate and the actuators, though the control performances should not be adversely affected. In an open-loop scheme, the control was not related to phase. In a closed-loop case, the control was executed by tuning the amplitude ratio and the phase shift between output and input of the controller, leading to the phase shift to be corrected.

An external control system is needed to control the motion of the actuators. Both open- and closed-loop control methods are deployed, as indicated schematically in Fig. 2(b). For the open-loop method, the actuators are simultaneously activated by a signal with controllable frequency and voltage, i.e. the perturbation frequency

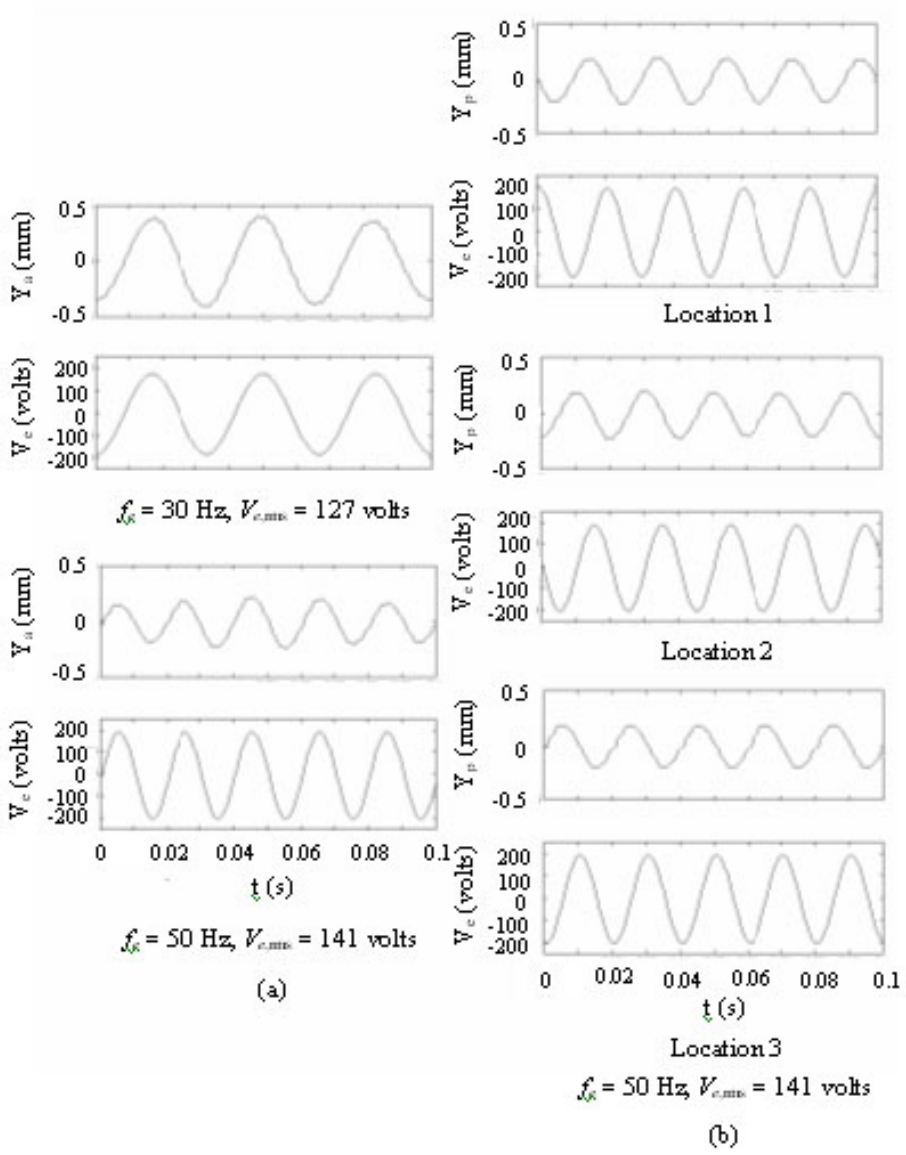

Figure 3. Typical time histories of actuator displacement signal Y_a, perturbation displacement signal Y_p and the corresponding excitation signal under different excitation frequency f_e and root mean square value of excitation voltage $V_{e,rms}$: (a) the perturbation surface was removed; (b) the perturbation surface was replaced.

f_p and perturbation voltage, generated by a signal generator. For the closed-loop scheme, they are activated by feedback signals from a system. The feedback control system may take the instantaneous signals from the individual lateral structural vibration Y or streamwise flow velocity u, or the combined Y and u for feedback signals, referred to as one-element and two-element control schemes, respectively. The structural vibration and the flow velocity may be measured using a laser vibrometer and a single hot wire, respectively. After being amplified, the feedback signals are filtered and then sampled into a controller based on a dSPACE control platform for real-time data processing. The output signals of the controller are filtered and amplified again before being used to drive the THUNDER actuators. For each control scheme, the aim is to effectively control flow or structural vibration or both, which was achieved by tuning the parameters of the controller. Each tuning process finally led to an optimal configuration with corresponding optimal parameters.

3 Applications

3.1 Control of One-degree-of-freedom Flow-induced Vibration

The perturbation-based control technique was first applied to the open-loop control of a resonant fluid-structure system, where the vortex shedding frequency was synchronized with the natural frequency, f_n', of an oscillating square cylinder [15]. The choice of this case study was because, under resonance, flow-induced vibration will be greatly enhanced, causing serious problems and even structural damages. The cylinder, flexibly supported at both ends, was allowed to vibrate only in the lift direction. Three actuators were embedded underneath one side, parallel to the flow, of the cylinder. They were simultaneously activated by a sinusoidal wave, thus forcing the cylinder surface to oscillate. As the normalized perturbation frequency f_p^* (asterisk denotes the normalization of f_p by the cylinder height, h, and the free-stream velocity, U_∞) was outside the possible synchronization range ($0.8f_s \sim 2f_s$) [26], i.e. $f_p^* = 0.11 \sim 0.26$, structural vibration (Y), vortex circulation (Γ) and mean drag coefficient ($\overline{C}_D$) were reduced by up to 75%, 50% and 21%, especially at $f_p^* = 0.1$. On the other hand, as f_p^* fell within the synchronization range, both Γ and $\overline{C}_D$ were increased; at $f_p^* = 0.13$, Γ was doubled and $\overline{C}_D$ grew by 35%.

The open-loop control suffered from two major drawbacks. First, the effective frequency range to achieve the desired performance was relatively narrow. Second, the energy required to drive the actuators was rather high. To resolve the problems, the closed-loop control method was introduced [27]. Two one-element control schemes and one two-element control scheme were deployed. The feedback signal of the former was either structural vibration Y (Y_control scheme) or fluctuating flow velocity u (u_control scheme) and that of the latter was a combination of Y and u ($u + Y$_control scheme). The Y_control scheme or u_control scheme did not necessarily perform better than the open-loop control. However, the $u + Y$_control led to almost completely destroying the Kámán vortex street and a 82% reduction in Y, 65% in Γ and 35% in $\overline{C}_D$, greatly outperforming the open-loop control. This

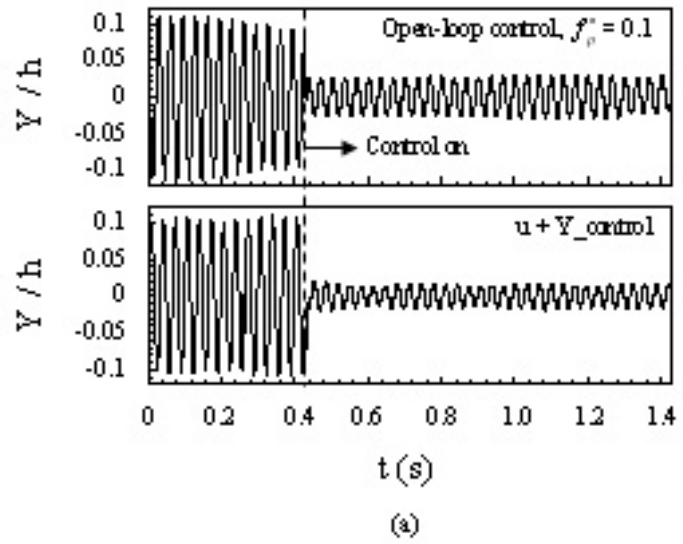

(a)

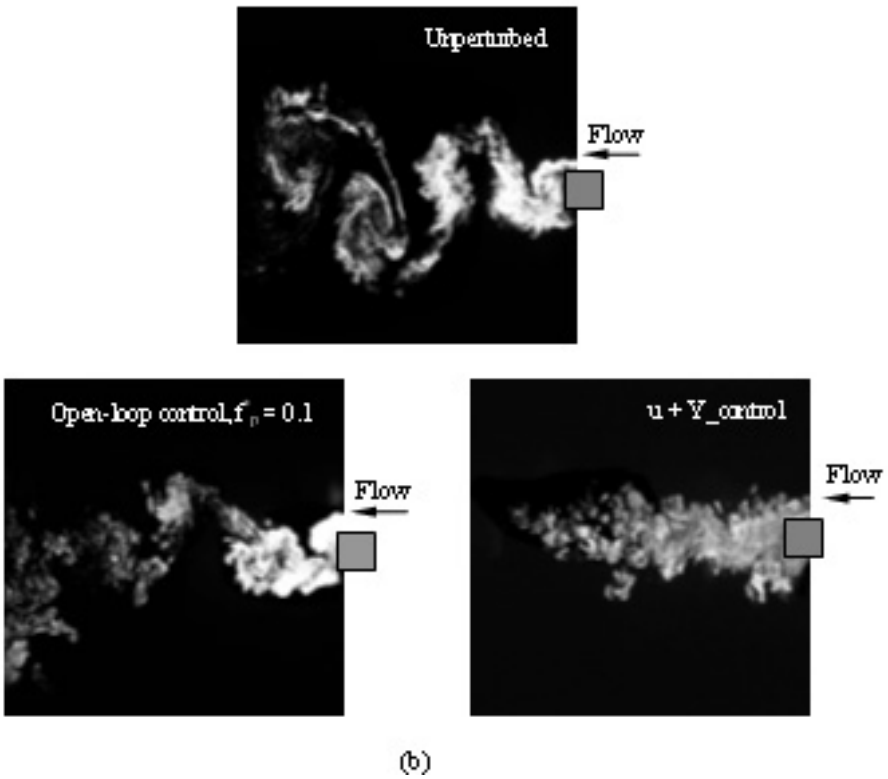

(b)

Figure 4. Control effect on structural vibration Y (a) and flow (b) when the control of fluid-structure interaction on a flexible supported rigid cylinder was investigated.

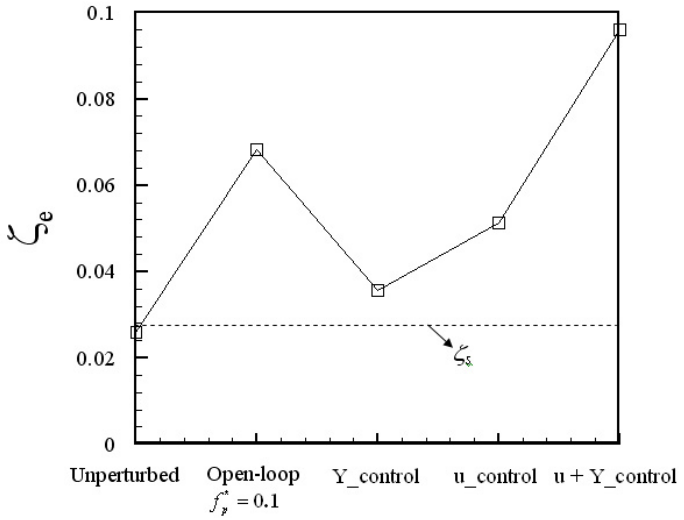

Figure 5. Effect of open- and closed-loop control on fluid-structure system damping ratios, ζ_e. The dash line denotes the structural damping ratio ζ_s measured without flow.

is illustrated by a comparison between the open-loop control ($f_p^* = 0.1$) and the $u + Y$_control in terms of the control effect on structural vibration [Fig. 4(a)] and flow [Fig. 4(b)]. The observation suggests that the proper choice of the feedback signal is crucial. It should be mentioned that the decreased Y was attributed to the modification of the fluid-structure system damping ratio ζ_e, defined as the sum of structural damping (ζ_s) and fluid damping (ζ_f). Figure 5 presents ζ_e under different control schemes, calculated using an auto-regressive moving average (ARMA) technique from time series of Y [28]. The ARMA model with an order of 190 and 70000 data points were used for calculation. Without perturbation, vortex shedding synchronizes with structural vibration, and ζ_e was less than ζ_s, albeit slightly, suggesting a negative ζ_f since $\zeta_e = \zeta_f + \zeta_s$. The negative ζ_f simply means that vortex shedding enhances the structural vibration. For the open-loop control, ζ_e increases by 163.2%, compared with the unperturbed. Similarly, the closed-loop control using the Y_control, u_control and $u + Y$_control leads to an increase in ζ_e by 37.9%, 97.7% and 271.4%, respectively, resulting in effective reduction in Y.

3.2 Control of Multiple-degree-of-freedom Flow-induced Vibration

The perturbation-based control technique was applied to control the fluid-structure interaction on a multi-freedom flexible structure. Closed-loop control of vortex and its induced vibration on a flexible square cylinder with fix supports at both ends were performed under resonance [29] and non-resonance conditions [30], respec-

tively. Five control schemes were investigated based on the feedback signals from either individual or combined responses of structural vibration (Y or dynamic strain ε_y in the lift direction) and u. Under resonance, f_s coincided with the first-mode natural frequency of the fluid-structure system. Experimental results showed that, irrespective of the control schemes, not only the first mode but also the higher-order mode oscillations were effectively attenuated. The best performance was achieved using the $u + Y$_control scheme, which almost completely destroyed vortex shedding, resulting in an 85% reduction in Γ and a 65% reduction in the amplitude of Y. Similar control effects were also observed for the non-resonant case.

3.3 Control of Blade-vortex Interaction

The perturbation-based control technique has been applied to modify the blade-vortex interaction (BVI) and to suppress the BVI noises commonly occurring in rotorcrafts, such as helicopters, turbo-machines and fans. This kind of noise is believed to be induced by an unsteady flow pressure during the process of the interaction between incident vortices and the leading edge of a hard-surfaced body such as an airfoil [31-33]. Considering the difficulty in directly measuring the BVI noise, the origin of the noise, i.e. the fluctuating flow pressure p at the leading edge of the body, was used as the control target [34]. A circular cylinder was used as the vortex generator. A NACA0012 airfoil was placed downstream with an angle of attack of 0^o. Piezo-ceramic actuators were installed near the leading edge of the airfoil. Two closed-loop control schemes were examined, which deployed p and flow velocity u near the airfoil leading edge as the feedback signal, respectively. Experimental results indicated that the control scheme based on u led to 40% impairment in Γ of the oncoming vortices and a simultaneous reduction in p by 39%, outperforming the control scheme based on p.

The overall performances of the open- and closed-loop control schemes in various control cases are summarized and compared in Tables 1-3. Note that the input energy E, approximately given by $E = 2\pi f_s C V_p^2$ [35], to the actuators is a good criterion for quantifying the control efficiency of various control schemes. Here C and V_p stand for the total capacitance of the actuators and the perturbation voltage exerted on the actuators, respectively. Obviously, all the results unequivocally demonstrate the effectiveness of the perturbation-based control on controlling the fluid-structure interaction on a cylinder. Among one-element schemes, the one using the feedback signal reflecting the excitation origin of fluid-structure interaction has better control performances. Furthermore, two-element control schemes, despite smaller E, outperform one-element control schemes and also the optimal open-loop control scheme, indicating the superiority of the two-element control scheme over others in terms of both control performances and efficiency.

Variables	Open-loop $f_p^* = 0.1$	u_control	Y_control	u+Y_control
Y_{rms}	75% ↓	53% ↓	40% ↓	82% ↓
u_{rms}	68% ↓	32% ↓	17% ↓	70% ↓
Γ	50% ↓	34% ↓	22% ↓	65% ↓
$\overline{C}_D$	21% ↓			35% ↓
E(J)	0.34	0.038	0.12	0.012

Table 1: Control performances of various control schemes when fluid-structure interaction on a flexible supported rigid cylinder is investigated.

4 Physical Mechanisms

Insight may be gained into the underlying physical mechanisms of the perturbation-based control by examining how the perturbation, flow and structure interact with each other. To this end, the effect of the perturbation on the flow was investigated. In order to separate the perturbation motion from that of cylinders, the closed-loop control of a stationary cylinder wake was conducted [36]. Figure 6 shows the variation of a typical spectral phase $\phi_{Y_p u_2}$ between the perturbation displacement Y_p and the streamwise flow velocity u_2, measured at a location where the main characteristics of vortex shedding may be reflected. The spectral phase between signals α_1 and α_2 is defined as $\phi_{\alpha_1\alpha_2} \equiv \arctan Q_{\alpha_1\alpha_2}/Co_{\alpha_1\alpha_2}$ and calculated using a Fast Fourier Transform (FFT) method [37], where $Q_{\alpha_1\alpha_2}$ and $Co_{\alpha_1\alpha_2}$ stand for the cospectrum and quadrature spectrum, respectively. Obviously, the control results in a $\phi_{Y_p u_2}$ of either about zero over a very large frequency range or -π over a small range of frequencies around f_s^*. As demonstrated in Zhang et al [36], $\phi_{Y_p u_2}$ is equivalent to the phase shift between the velocity ($\dot{Y}_p$) of the perturbation surface and the lateral velocity component (v) of flow around the structure. Therefore, $\phi_{Y_p u_2} = 0$ means in-phased $\dot{Y}_p$ and v, which promotes the roll-up motion of vortices and subsequently the vortex strength. On the other hand, $\phi_{Y_p u_2} = -\pi$ at f_s^* means anti-phased $\dot{Y}_p$ and v which is associated with vortex shedding, that is, the surface perturbation created by actuators clashes with the flow in the lateral direction. The opposite or collided movement between $\dot{Y}_p$ and v is responsible for the greatly impaired vortex strength behind the cylinder [Fig. 4(b)].

From a different perspective, $\phi_{Y_p u_2}$ also roughly represents the phase relation between the two components of the force F'_y of structure acting on flow in the lateral direction [36], i.e. the unperturbed component $F'_{y,u}$, due to the structural surface without perturbation, and the perturbation component $F'_{y,p}$, due to the local surface perturbation activated by the actuators. The three force vectors satisfy the relation $F'_y = F'_{y,u} + F'_{y,p}$. Thus, $\phi_{Y_p u_2} = 0$ (the enhanced vortex strength case) corresponds to in-phased $F'_{y,u}$ and $F'_{y,p}$, leading to an increase in F'_y. On the other hand, $\phi_{Y_p u_2} = -\pi$ (the impaired vortex strength case) corresponds to anti-phased $F'_{y,u}$ and $F'_{y,p}$, resulting in a decrease in F'_y. This provides a physical explanation about the alteration in the vortex strength. In addition, results reported in [36] also showed that similar

Variables	u_control	ε_y_control	Y_control	u+ϵ_y_control	u+Y_control
Y_{rms}	24% ↓	43% ↓	47% ↓	63% ↓	71% ↓
$\varepsilon_{y,rms}$	25% ↓	38% ↓	40% ↓	57% ↓	65% ↓
u_{rms}	37% ↓	29% ↓	36% ↓	54% ↓	63% ↓
Γ	47% ↓	48% ↓	54% ↓	74% ↓	85% ↓
$\overline{C}_D$					30% ↓
E(J)	0.19	0.15	0.11	0.065	0.049

Table 2: Control performances of various control schemes when fluid-structure interaction on a fix supported flexible cylinder is investigated under resonance case.

Variables	p_control	u_control
u_{rms}	18% ↓	21% ↓
Γ	31% ↓	40% ↓
p_{rms}	30% ↓	39% ↓
E(J)	0.037	0.016

Table 3: Control performances of various control schemes when blade-vortex interaction (BVI) on an airfoil is investigated .

control effects were obtained as Re varied within a range, suggesting the control technique possessed a certain degree of adaptiveness and robustness.

The modified vortex strength by the perturbation effect will undoubtedly influence interactions between flow and structure since a coupled relationship between them exists. As an example, the impaired case can be inferred from the spectral phase ϕ_{Yu_2} between Y and u_2 with and without control (Fig. 7). Let us further examine ϕ_{Yu_2} when the resonant fluid-structure interaction with a rigid cylinder flexibly supported was perturbed. Note that the relationship between Y and u_2 at f_s^* equivalently describes that between $\dot{Y}$ and v around the structure [15]. In the absence of perturbation, ϕ_{Yu_2} is zero over a range of frequencies about f_s^*, implying that the unperturbed flow strongly synchronized with the oscillation of the cylinder. However, in case of the open-loop control ($f_p^* = 0.1$) or the closed-loop control such as the $u + Y$_control, ϕ_{Yu_2} is altered from 0 to -π over a range of frequencies around f_s^*, suggesting that the synchronizing relationship between flow and structure is significantly modified; the synchronized flow and structure now collided or acted against each other, implying effectively impaired fluid-structure interaction. The spectral coherence $Coh_{\alpha_1\alpha_2} = (Co^2_{\alpha_1\alpha_2} + Q^2_{\alpha_1\alpha_2})/E_{\alpha_1}E_{\alpha_2}$ provides a measure of the degree of correlation between the Fourier components of α_1 and α_2[37]. Under no control condition, the peak in Coh_{Yu_2} (Fig. 8) at f_s^* reaches about 0.66, suggesting a strong correlation between flow and structure, but recedes by 77% under the open-loop control and by 83% under the $u + Y$_control; the coupled relationship between flow and structure is remarkably weakened.

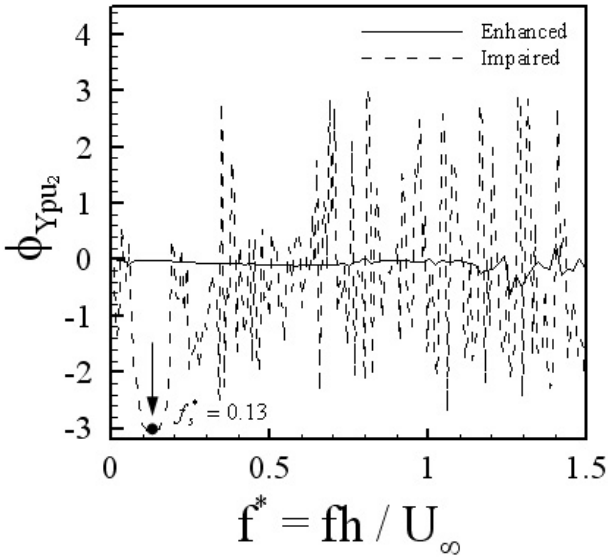

Figure 6. Typical spectral phase $\phi_{Y_p u_2}$ between the perturbation displacement (Y_p) and the streamwise flow velocity (u_2) under control.

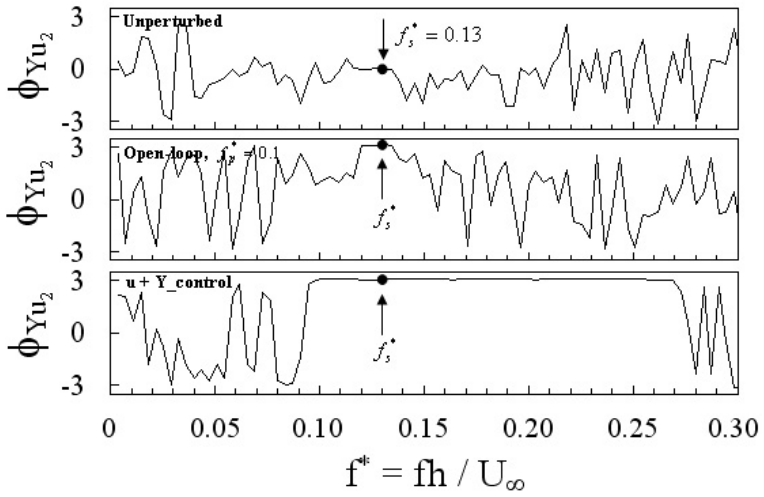

Figure 7. Typical spectral phases ϕ_{Yu_2} between the structural vibration (Y) and the streamwise flow velocity (u_2) reflecting fluid-structure interaction with and without control.

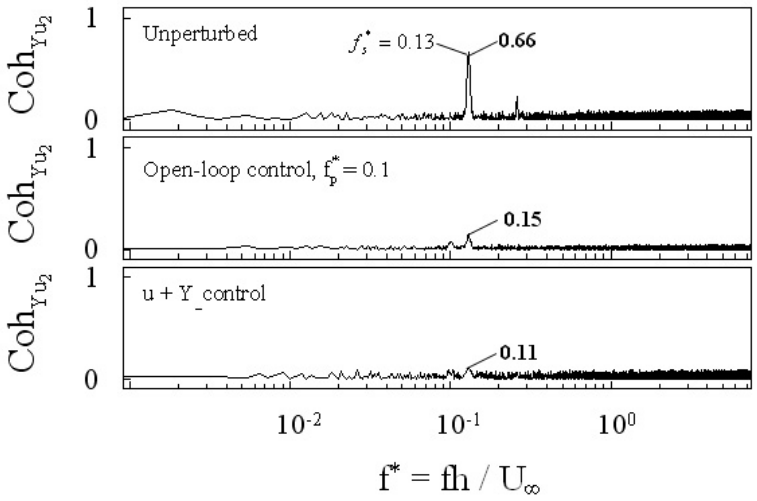

Figure 8. Typical spectral coherences Coh_{Yu_2} between the structural vibration (Y) and the streamwise flow velocity (u_2) reflecting fluid-structure interaction with and without control.

Based on the above analyses, an interpretation for the control mechanism of the perturbation-based control is now proposed. Vortex-induced vibration originates from fluid-structure interactions. The open- or closed-loop controlled perturbation on the structural surface may modify the nature of the interaction between flow and structure, either reinforcing or weakening each other, and acting to promote or downgrade the strength of vortical flow nearby. Physically, this corresponds to the enhancement and impairment of the force acting on the flow exerted by the structure, respectively. The modified vortex strength has a profound impact upon fluid-structure interactions.

The differences in the control performances of open- and closed-loop control schemes are attributed to different control signals, which are used to drive actuators. In the open loop, the perturbation signal is independent of flow, interactions between the flow and the structure are sensitive to the frequency of f_p^*. Depending on whether f_p^* is within or outside the synchronization range, the coupled fluid-structure interaction may be either enhanced or weakened. For the closed-loop control, the feedback signal is the control signal. The one-element control schemes use the signal of either structural vibration or flow velocity for the feedback signal. Among the choices of the feedback signals, the one containing the excitation source of fluid-structure interactions has best performances. The feedback signal in one-element schemes contains only part of the information of fluid-structure interactions. Consequently, the control performance of one-element schemes is limited. On the other hand, flow-structure interactions are well reflected in the feedback signal of the two-element schemes. For example, the $u + Y$_control utilizes a combination of flow and structural vibration as the feedback signal, which reflects the interaction/coupling

between flow and structural vibration. As a result, the two-element schemes exhibit superiority over the one-element schemes in terms of control performance and efficiency.

5 Summary

This paper reviews the recent progress made on the control of fluid-structure interaction based on a novel surface-perturbation technique, summarizing the major issues, including the implementation of the technique, different control schemes, control performances, various applications and the underlying mechanism. The issues are important in using this technique and expanding its use into new applications in the future.

6 Acknowledgements

The authors wish to acknowledge support given to them by Research Grants Council of Hong Kong Special Administrative Region, China (Project Nos. PolyU 5294/03E and PolyU1/02C). A special fund for recently promoted Chair Professors given by The Hong Kong Polytechnic University is also acknowledged.

7 References

[1] H. Schlichting, Boundary-layer Theory, McGraw-Hill, New York, 1979.

[2] O.M. Griffin and S.E. Ramberg, On vortex strength and drag in bluff-body wakes, *J. Fluid Mech.*, **69**, (1975) 721-728.

[3] T. Sarpkaya, Vortex-induced oscillations-A selected review, *J. Appl. Mech.*, **46**, (1979) 241-258.

[4] M.S. Howe, Acoustics of Fluid-Structure Interactions, Cambridge University Press, UK, 1998.

[5] M.M. Zdravkovich, Review and classification of various aerodynamic and hydrodynamic means for suppressing vortex shedding, *J. Wind Eng. Ind. Aerod.*, **7**, (1981) 145-189.

[6] J.C. Owen, P.W. Bearman and A.A. Szewczyk, Passive control of viv with drag reduction, *J. Fluid Struct.*, **15**, (2001) 597-605.

[7] R.D. Blevins, The effect of sound on vortex shedding from cylinders, *J. Fluid Mech.*, **161**, (1985) 217-237.

[8] K. Roussopoulos, Feedback control of vortex shedding at low Reynolds numbers, *J. Fluid Mech.*, **248**, (1993) 267-296.

[9] J.E. Ffowcs-Williams and B.C. Zhao, The active control of vortex shedding, *J. Fluid Struct.*, **3**, (1989) 115-122.

[10] H.M. Warui and N. Fujisawa, Feedback control of vortex shedding from a circular cylinder by cross-flow cylinder oscillations, *Exp. Fluids*, **21**, (1996) 49-56.

[11] P.T. Tokumaru and P.E. Dimotakis, Rotary oscillation control of a cylinder wake, *J. Fluid Mech.*, **224**, (1991) 77-90.

[12] D.R. Williams, H. Mansy and C. Amato, The response and symmetry properties of a cylinder wake subjected to localized surface excitation, *J. Fluid Mech.*, **234**, (1992) 71-96.

[13] A. Baz and M. Kim, Active modal control of vortex-induced vibrations of a flexible cylinder, *J. Sound Vib.*, **165**, (1993) 69-84.

[14] J. Tani, J. Qiu and Y. Liu, Robust control of vortex-induced vibration of a rigid cylinder supported by an elastic beam using -synthesis, *J. Fluid Struct.*, **13**, (1999) 865-875.

[15] L. Cheng, Y. Zhou and M.M. Zhang, Perturbed interaction between vortex shedding and induced vibration, *J. Fluid Struct.*, **17**, (2003) 887-901.

[16] P.W. Bearman, On vortex street wakes, *J. Fluid Mech.*, **28**, (1967) 625-641.

[17] M. Provansal, C. Mathis and L. Boyer, Benard-von Kámán instability: transient and forced regimes, *J. Fluid Mech.*, **182**, (1987) 1-22.

[18] F.B. Hsiao and J.Y. Shyu, Influence of internal acoustic excitation upon flow passing a circular cylinder, *J. Fluid Struct.*, **5**, (1991) 427-442.

[19] X.Y. Huang, Feedback control of vortex shedding from a circular cylinder, *Exp. Fluids*, **20**, (1996) 218-224.

[20] J.P. Den Hartog, Mechanical Vibrations, McGraw-Hill, New York, 1947.

[21] R. Parker, Resonance effects in vortex shedding from parallel plates, some experimental observations, *J. Sound Vib.*, **4**, (1966) 62-72.

[22] J.P. Marouz and L. Cheng, A feasibility study of active vibration isolation using THUNDER actuators, *Smart Mater. Struct.*, **11**, (2002) 854-862.

[23] J.L. Pinkerton and R.W. Moses, A Feasibility study to control airfoil shape using THUNDER, NASA Technical Memorandum 4767, 1997.

[24] V. Jayachandran, N.E. Meyer, M.A. Westervelt and J.Q. Sun, Piezoelectrically driven speakers for active aircraft interior noise suppression, *Appl. Acoustics*, **57**, (1999) 263-277.

[25] B.M. Copeland, J.D. Buckley, R.G. Bryant, R.L. Fox and R.F. Hellbaum, THUNDER - an ultra-high displacement piezoelectric actuator, NASA Langley Research Center. Hampton, VA, 23681-0001, 1999.

[26] B.H.L. Gowda, Some measurements on the phenomenon of vortex shedding and induced vibrations of circular cylinders, Deutsche Luft- und Raumfahrt Forschungsbericht, (1975) No. 75-01.

[27] M.M. Zhang, L. Cheng and Y. Zhou, Closed- loop-controlled vortex shedding from a flexibly supported square cylinder under different schemes, *Phy. Fluids*, **16**, (2004) 1439-1448.

[28] Y. Zhou, Z.J. Wang, R.M.C. So, S.J. Xu and W. Jin, Free vibrations of two side-by-side cylinders in a cross flow. *J. Fluid Mech.*, **443**, (2001) 197-229.

[29] L. Cheng, Y. Zhou and M.M. Zhang, Controlled vortex-induced vibration on a fix-supported flexible cylinder in crossflow, *J. Sound Vib.*, (2006) (In press).

[30] M.M. Zhang, L. Cheng and Y. Zhou, Control of vortex-induced non-resonance vibration using piezo-ceramic actuators embedded in a structure, *Smart Mater. Struct.*, **14**, (2005) 1217-1226.

[31] S. Ziada and D. Rockwell, Vortex-leading-edge interaction, *J. Fluid Mech.*, **118**, (1982) 79-107.

[32] J.C. Hardin and S.L. Lamkin, Concepts for reduction of blade/vortex interaction noise, *J. Aircr.*, **24**, (1987) 120-125.

[33] D. Rockwell, Vortex-body interactions, *Annu. Rev. Fluid Mech.*, **30**, (1998) 199-229.

[34] M.M. Zhang, L. Cheng and Y. Zhou, Closed-loop control of vortex-airfoil interaction noise, Fourth Conference on Bluff Body Wakes and Vortex-Induced Vibrations, ID-78, Santorini, Greece, 21-24 June, 2005.

[35] L.K. Baxter, Capacitive Sensors: Design and Applications, IEEE press, New York, 1997.

[36] M.M. Zhang, L. Cheng and Y. Zhou, Closed-loop manipulation of vortex shedding from a fixed-supported square cylinder, *Exp. Fluids*, **39**, (2005) 75-85.

[37] H.J. Zhang, Y. Zhou and R.A. Antonia, Longitudinal and spanwise structures in a turbulent wake, *Phy. Fluids*, **12**, (2000) 2954-2964.